Tellurium and selenium sorption kinetics and solid fractionation under contrasting estuarine salinity and turbidity conditions

Teba Gil-Díaz, Jörg Schäfer, Virginia Keller, Elisabeth Eiche, Lionel Dutruch, Claudia Mössner, Markus Lenz, Frédérique Eyrolle

Tellurium and selenium sorption kinetics and solid fractionation under contrasting estuarine salinity and turbidity conditions

Teba Gil-Díaz[a], Jörg Schäfer[a]*, Virginia Keller[b], Elisabeth Eiche[b], Lionel Dutruch[a], Claudia Möβner[b], Markus Lenz[c], Frédérique Eyrolle[d]

[a]*Université de Bordeaux, UMR CNRS 5805 EPOC, NB18, Allée Geoffroy Saint-Hilaire, 33615 Pessac, France;* [b]*Institute of Applied Geosciences, Karlsruhe Institute of Technology (KIT), Adenauerring 20b, 76131 Karlsruhe, Germany;* [c]*Institute for Ecopreneurship, University of Applied Sciences and Arts Northwestern Switzerland (FHNW), School of Life Sciences, Gründenstrasse 40, 4132 Muttenz, Switzerland;* [d]*Institut de Radioprotection et de Sûreté Nucléaire (IRSN), PSE-ENV/SRTE/LRTA,BP 3, 13115, Saint Paul Lez Durance, France*

*corresponding author: jorg.schafer@u-bordeaux.fr

Abstract

Tellurium (Te) is a Technology Critical Element (TCE) and a relevant product of nuclear fission. It has an unknown environmental biogeochemical cycle, mostly related to current analytical challenges in measuring its ultra-trace dissolved concentrations in complex environmental matrices. It is therefore generally compared to its geochemical pair selenium (Se), which shows a narrow range between diet essentiality and toxicity properties. Batch experiments using isotopically-labelled stable Te and Se were performed with fresh suspended particulate matter (SPM) from the fluvial part of the Gironde Estuary, simulating both estuarine salinity (S=0 vs S=32) and turbidity (100 mg L^{-1} vs 1000 mg L^{-1}) gradients to understand the importance of the particulate phases in Te reactivity under estuarine conditions and verify the resemblance to Se behaviour. These experiments addressed sorption kinetics, sorption isotherms and fractionation from selective extractions of final equilibrated SPM. Results showed a strong, salinity-independent affinity of Te for the particulate phases (log_{10} Kd ~ 4.9 L kg^{-1}), following a Langmuir-type isotherm. Contrastingly, Se adsorbs clearly less to estuarine SPM (log_{10} Kd ~ 2.5 L kg^{-1}), following a Freundlich-type isotherm. Both isotherms and selective extractions highlighted differences between Te and Se sequestration. Selective extractions suggested higher mobility of particulate Se in contrast to Te. Based on these results the paper sets a first dispersion scenario on the environmental fate of radioactive Te and Se after hypothetical nuclear power plant accidental releases in coastal aquatic systems such as the Garonne-Gironde fluvial-estuarine system.

Keywords: technology critical elements, isotherms, selective extractions, distribution coefficient (Kd), Te environmental cycle, radionuclide releases

1. Introduction

Radioactive tellurium (Te) is produced during nuclear fission reactions in non-negligible quantities. All Te radionuclides have a 13-16% probability of being produced from ^{239}Pu- and ^{235}U-based fuels compared to ~11% for Cs and ~10% for I radionuclides (unpublished data calculated from Element Collection Inc. and Sonzogni 2013). There is little information on the specific Te species released from nuclear power plant (NPP) accidents, potentially presenting both (i) volatile/intermediate (Morewitz 1981), and (ii) refractory character (e.g., forming metal/oxide compounds; Kleykamp 1985; Izrael 2002 and references therein). Though different NPP accidents display different emission patterns, Te radionuclides were released into the environment during both April-1986 Chernobyl (CNPP) and March-2011 Fukushima Daiichi (FDNPP) accidental events (Steinhauser et al. 2014). In these cases, short-term half-life Te radionuclides (e.g., ^{132}Te half-life of 3.2 days) produced important atmospheric radioactive emissions (^{132}Te: ~1150 PBq at CNPP and ~180 PBq at FDNPP) comparable to ^{137}Cs and ^{131}I, the most monitored radionuclides after NPP accidental events (~85 PBq and ~1700 PBq at CNPP, ~37 PBq and ~160 PBq at FDNPP, respectively; Steinhauser et al. 2014). Emitted Te radionuclides were still detected in the atmosphere one month after the FDNPP accident reflecting their non-negligible environmental persistence and potential worldwide atmospheric dispersion (Baeza et al. 2012; Ishikawa et al. 2014; Leppänen et al. 2013). In fact, radioactive Te has been detected in FDNPP fallouts (Saegusa et al. 2013) and in seawater from Monaco, after CNPP (May 1986), yet with relatively low ^{129}Te activities in the dissolved (0.13 Bq L^{-1}) and particulate (1.18 mBq L^{-1}) phases (Whitehead et al. 1988). The latter study further suggested for the first time the moderate particle-reactive behaviour of radioactive Te and its potential intake by marine bivalves, thus, risk of entering environmental food chains (i.e., up to 340 Bq kg^{-1} DW in mussel soft tissues; Whitehead et al. 1988).

On the other hand, radioactive selenium (Se) is a widely known fission product of nuclear reactions. It can be released into the environment during several steps of the nuclear fuel cycle comprising NPP wastewaters and spent nuclear fuel, with recent research focusing specifically on ^{79}Se mobility (half-life of ~10^5 y) from waste storage and nuclear waste disposal areas (Aguerre and Frechou 2006; Asai et al. 2011; Hamed et al. 2017). Selenium is considered a highly soluble, mobile, biologically essential and toxic trace element with a more comprehensive biogeochemical cycle (e.g., Tan et al. 2016; Winkel 2016) than that of Te. Due to their overall chemical similarity (both chalcogens/Group 16 elements), the environmental behaviour of Te is generally assumed to be similar to that of Se (Belzile and Chen 2015).

Given the massive dispersion of past NPP accidental releases through both aquatic and atmospheric compartments, the development of management plans for hypothetical future accidental NPP events requires knowledge on radionuclide behaviour including adsorption kinetics under environmentally-representative conditions. Worldwide, many NPPs are located on fluvial-estuarine systems, for which little is known on Te (Wu et al. 2014; Duan et al. 2014; Biver et al. 2015) and Se (Measures and

Burton 1978; Cutter 1989; Bizsel et al. 2017) environmental dispersion and biogeochemical behaviour.

This study aimed at determining Te and Se reactivity in estuarine salinity and turbidity gradients through isotopically-labelled sorption experiments (kinetics and isotherms) using natural bulk sediments and natural water matrices. Parallel selective extractions of particles previously exposed to isotopically-labelled Te and Se address solid fractionation for both, inherited and spiked concentrations. The results were further compared to dynamic environmental conditions (i.e., environmental timescales of semi-diurnal tidal variations, seasonal migration of the estuarine maximum turbidity zone, etc.). This comparison allowed to assess and predict for the first time the environmental fate and potential dispersion of short-lived Te vs long-lived Se radionuclides in case of a hypothetical accidental NPP liquid discharge in the fluvial-estuarine system of the Gironde Estuary (SW France hosting two NPPs: the Blayais NPP and the Golfech NPP, Gil-Díaz et al. 2018).

2. Material and Methods

2.1. Experimental design

Sorption experiments simulated four experimental conditions representative of the Gironde Estuary salinity and turbidity gradients: two contrasting water matrices (salinities 0 and 32) and two solid/liquid ratios (100 mg L^{-1} and 1000 mg L^{-1} DW). Freshwater from the Garonne River and seawater from the Arcachon Bay, were filtered with 0.45 µm Teflon filters (FHLC, Merck Millipore Ltd.). Freshwater sediments were sampled at Portets (~30 km upstream from Bordeaux) on the Garonne River. The water content was evaluated by comparing the masses of precise volumes of wet and dry sediment aliquots.

Spike solutions were prepared by dissolution of elemental ^{125}Te (99.89% purity; Cortecnet, France) and ^{77}Se (99.20% purity; Cortecnet, France) in HCl (2% Suprapur®, Merck) and HNO_3 (2% Suprapur®, Merck), respectively, heated at 70ºC until dissolution. This method is known to produce oxidized species, i.e., well-known reaction for the formation of Se(VI) (Van Dael et al. 2004). Isotopically-labelled Te and Se solutions were further oxidised with H_2O_2 (30 µL L^{-1} 30% J.T. Baker ultrapure) in the different water matrices to favour the oxidation state of $^{125}Te(VI)$ and $^{77}Se(VI)$ (e.g., Edwards et al. 1959; Horner and Leonard 1952), followed by an equilibration period of 24h. Slurries were prepared from the fresh sediments and unspiked water matrices and equilibrated during 24h, to avoid potential effects of sediment-water interactions during the sorption experiment (e.g., other ionic exchanges related to matrix properties influencing spiked Te or Se adsorption).

Sorption kinetics were performed with nominal concentrations of 5 µg L^{-1} of $^{125}Te(VI)$ and 100 µg L^{-1} of $^{77}Se(VI)$. These spike concentrations are higher than those expected in most natural systems but

were required for analytical purposes. All sorption experiments were performed in acid-washed 50 mL centrifuging polypropylene (PP) tubes with 3 replicates per experimental condition. Sorption experiments were placed on an automatic overhead shaker (REAX 20 Heidolph Instruments) and sampled at t = 0, 2, 4, 8, 24 and 48h (N=3). These relatively short-term experimental conditions are considered to be in accordance with the environmental timescales of highly dynamic environments such as those occurring in continent-ocean transition systems. Temperature (21.1 ± 0.4 ºC), pH (7.50 ± 0.45) and oxic (104 ± 0.5% saturation) conditions, were monitored and remained stable throughout the experiment. In parallel, blank tubes containing only spiked water solutions were used to control ^{125}Te and ^{77}Se potential losses onto PP walls over time.

Adsorption isotherms were performed for two SPM concentrations (100 mg L^{-1} and 1000 mg L^{-1}) with initial concentrations of dissolved ^{125}Te of 0.1, 0.25, 0.5, 1, 2.5, 5 µg L^{-1} and initial concentrations of dissolved ^{77}Se of 0.5, 5, 10, 25, 50, 75, 100 µg L^{-1} (N=2) and sampled after 48h. Due to analytical constraints (i.e., salt tolerance of the ICP-MS), especially at the low concentration ranges, these experiments were only performed in freshwater conditions.

In both kinetics and isotherm experiments, dissolved Te (Te_d) and dissolved Se (Se_d) were monitored. Particulate concentrations were only determined for isotherm experiments using freshwater slurries with 1000 mg L^{-1} SPM for mass balance calculations. In all cases, the dissolved phase was separated from the particulate phase by centrifugation (10 min at 4000 rpm; Hettich Rotofix 32A centrifuge) and filtered (0.2 µm Minisart® cellulose acetate) into acid-washed PP 15 mL tubes. These were then acidified with HNO_3 (1/1000 v/v; J.T. Baker ultrapure, 14 M) and stored at 4ºC in the dark until analysis.

2.2. Parallel selective extractions and total digestions

High SPM concentrations (2 - 4 g L^{-1} DW) in freshwater (S = 0) and seawater (S = 32) were left to equilibrate for 48h in spiked solutions of nominal 10 µg L^{-1} of ^{125}Te and 100 µg L^{-1} of ^{77}Se. All sediments were recovered by centrifugation (Hettich ROTOFIX 32A), oven dried (70ºC, constant weight) and grinded in agate mortars, then aliquoted and extracted with parallel selective extractions (two replicates per extraction mode, Table 1). The targeted operationally defined solid fractions were: F1 – easily exchangeable and/or carbonate fraction (acetate solution extracting carbonates, Mn oxyhydroxides, sulphates and organic matter phases; Bordas and Bourg 1998; Kersten and Förstner 1987), F2 – reducible Fe/Mn oxides (ascorbate solution extracting Mn oxide and amorphous Fe oxide phases; Kostka and Luther 1994), F3 – oxidisable fraction (H_2O_2 extraction of organic matter and labile/amorphous sulphide phases; Tessier et al. 1979; Ma et Uren 1995) and F4 – reactive and "potentially bioaccessible" fraction (HCl 1M acid extraction of amorphous and crystalline Fe and Mn oxides, carbonates, amorphous monosulphurs and phyllosilicate phases; Huerta-Díaz and Morse 1990;

Gasparon and Matschullat 2006). In addition to the latter, acid extraction with HNO_3 1 M (F4N) was performed on a separate aliquot to discard the Cl effect or specific acid effect on F4 obtained from HCl 1 M leaching. All reagents used were of high purity grade except H_2O_2 (p.a. grade). High Te contamination of ~35 µg L^{-1} was observed in the extraction blanks of F3 potentially from the H_2O_2 solution or the added ammonium acetate. This contamination is suspected to have been adsorbed into other than H_2O_2-extracted solid fractions (given the Te behaviour, see results), thus not affecting the inherited Te identified in F3 fraction. All extractions were performed in acid-washed (HNO_3 10%) PP Falcon 50 mL conical centrifuge tubes (Fisher Scientific). Three blanks of each extraction were performed. Currently, no Certified Reference Materials (CRM) are available for Te and Se selective fractions. Residual fractions were calculated as the difference between the acid-soluble fraction (F4 or F4N) and the total adsorbed particulate concentration.

Total sediment concentrations were determined differently for particulate Te (Te_p) and particulate Se (Se_p). Mineralisation of sediment for Te analysis was achieved using a tri-acid digestion with HNO_3 + HCl + HF as described elsewhere (e.g., Schäfer et al. 2002). Briefly, samples of 30 mg were digested in closed PP tubes (DigiTUBEs®, SCP Science) on a heating block (2 h at 110 ºC) using 750 µL HNO_3 (14 M Suprapur®, Merck), 1.5 mL HCl (10 M Suprapur®, Merck) and 2.5 mL HF (29 M Suprapur®, Fisher). After an evaporation step at 120ºC, re-dissolution of the samples was performed with 250 µL HNO_3 (14 M) and heating. After cooling, the samples were brought to 10 mL using Milli-Q water (18.2 MΩ).

For the analysis of Se_p (volatile at >70ºC, not compatible with the above-described tri-acid digestion) total microwave-assisted digestions (START 1500, MLS GmbH) were performed with 40 - 50 mg of sediment aliquots (Eiche et al. unpublished) already dried (50ºC drying oven) and homogenised (agate mortar). Briefly, 3 mL HNO_3 (sub-boiled acid-distilled 65%, p.a. grade, VWR Chemicals), 0.5 mL H_2O_2 (30% Rotipuran®, Carl Roth), 0.25 mL HF (40% Suprapur®, Merck KGAA Darmstadt) and 0.5 mL ultrapure Milli-Q water were added. The temperature program was: 18ºC min^{-1} to 75ºC, followed by 7ºC min^{-1} to 110ºC, then 8ºC min^{-1} to 150ºC and 6ºC min^{-1} to 210ºC, with a constant temperature of 210ºC during 10 min before completely cooling down over night. After digestion, samples were transferred into PTFE vessels and evaporated on a hotplate to dryness at 70ºC (no Se evaporation at this temperature), recovered with 270 µL of HNO_3 (65% Suprapur), heated at 70ºC for 1h and made up with ultrapure Milli-Q water to a final volume of 6 mL.

2.3. Tellurium quantification

Dissolved Te in samples from freshwater kinetics and isotherms experiments were directly analysed by ICP-MS (X-Series II, Thermo Fisher Scientific) using external calibration. Seawater matrices were diluted in 2% HNO_3 (J.T. Baker ultrapure, 14 M) and quantified with external

calibration in an adapted salty matrix. In all cases, recoveries were between 85 – 91% for NIST 1643f CRM (N=4) with a detection limit (LOD) of 0.01 µg L^{-1} (N=10). Given this LOD, the spiked concentrations and the dilution effect, it is assumed that pre-existing inherited ^{125}Te in the kinetics and isotherm samples is negligible in the water matrices as expected concentrations are in the range of 1 ng L^{-1} (Filella 2013; Belzile and Chen 2015). The latter is corroborated by upstream freshwater analyses (Gil-Díaz et al. 2019a).

Digestates of particles from the isotherm experiments using 1000 mg L^{-1} SPM in freshwater were quantified with an QQQ-ICP-MS (Agilent 8800, Basel, Switzerland) using an external calibration with ^{103}Rh as internal standard to correct for matrix effects. Tellurium was measured in oxygen-shift mode using O_2 as collision gas ($^{125}Te + {}^{16}O \rightarrow {}^{141}TeO$). A certified reference material (NCS 73307) was used for quality check-up of the total digestions showing mean ± SD recovery values of 94 ± 17% (N=3).

Particulate Te in total digestions and selective extractions were quantified by TripleQuad-ICP-MS (TQ ICP-MS; iCAP-TQ, Thermo®) using external calibration. Given the very low inherited Te_p concentrations (~0.04 mg kg^{-1}), natural/inherited Te (Te_{nat}) was quantified from ^{126}Te measured in KED-mode (He), correcting for $^{86}Sr^{40}Ar$, $^{110}Cd^{16}O$ and $^{110}Pd^{16}O$ interferences (Filella and Rodushkin 2018) with respective monoelemental solutions (influencing <0.1%) and ^{126}Xe from analytical blanks (2% HNO_3). Spiked/experimental ^{125}Te (Te_{ex}) was determined by TQ ICP-MS in mass-shift O_2-mode (iCAP-TQ, Thermo®). Certified reference materials were used for instrumental quality check-up (freshwater NIST 1643f) and total digestions (stream sediment NCS 73307). Recoveries were 95 ± 5% (N=5) in the KED-mode, 89 ± 10% (N=5) in the O_2-mode for NIST 1643f and 99 ± 14% (N=4) in the KED-mode and 70 ± 19% (N=4) in the O_2-mode for NCS 73307. Inherited Te was quantified from both Te-spiked SPM and Se-spiked SPM (i.e., no influence from potential ^{125}Te spike effect). In selective extractions, Te_{nat} concentrations ranged from 5-fold (in F2 extractions) to 200-fold (in F4 extractions) above LOD (0.1 ng L^{-1}, N=10).

2.4. Selenium quantification

Dissolved Se concentrations from sorption kinetics and isotherms were quantified by ICP-MS (XSeries 2, Thermo Fisher Scientific, KIT, Germany) using external calibration, CCT-mode (collision cell with He:H_2 mixture at 92%: 8% to minimise $^{40}Ar^{37}Cl$ interferences) and $^{103}Rh/^{115}In$ as internal standards. Analytical quality control was followed with certified drinking water (CRM-TMDW) and freshwater (NIST 1643f) standards showing recoveries ranging between 98 – 106% for the former (N=16) and 100-102% for the latter (N=16), with a LOD of 0.06 µg L^{-1} (N=10). Natural Se_d concentrations were 0.14 ± 0.03 µg L^{-1} in freshwater (N=32) and ~0.31 µg L^{-1} for seawater (unpublished).

Total ^{77}Se digestions from the 1000 mg L^{-1} SPM isotherm experiment were quantified by QQQ-ICP-MS (Agilent 8800, Basel, Switzerland) using external calibration with ^{103}Rh as internal standard and oxygen-shift mode collision gas for ^{77}Se ($^{77}Se + {}^{16}O \rightarrow {}^{93}SeO$) to avoid, amongst others, doubly charged Rare Earth Element (REE) interferences (mainly $^{154}Sm^{++}$, $^{154}Gd^{++}$). The CRM NCS 73307 showed recoveries of total digestions ranging from 70 to 134% (N=3).

Analyses of Se in selective extractions, namely particulate inherited/natural Se (Se_{nat}) and spiked/experimental Se (Se_{ex}) were quantified with the O_2-mode of the TQ ICP-MS (iCAP-TQ, Thermo®) using external calibration, eliminating the known polyatomic interferences (e.g., $^{40}Ar^{37}Cl$, $^{154}Sm^{++}$ and $^{154}Gd^{++}$ in ^{77}Se, ^{78}Kr, $^{156}Gd^{++}$ and $^{156}Dy^{++}$ in ^{78}Se, $^{81}Br^{1}H$ and ^{82}Kr in ^{82}Se) on both inherited (^{78}Se, ^{80}Se, ^{82}Se) and spiked (^{77}Se) isotopes. Particulate Se_{nat} was quantified from both Te-spiked and Se-spiked slurries. Analytical quality check showed recoveries of 95 ± 3% for NIST 1643f and 85 ± 2% for NIST 1640a. Total adsorbed Se_{ex} was calculated from the difference between initially spiked and final Se_d after 48h.

2.5. Distribution coefficient (Kd)

Tellurium and Se partitioning between dissolved and particulate concentrations was evaluated from the kinetic experiments at equilibrium by using the particle-water distribution coefficient (Kd), described in Sung (1995). Briefly, Kd (in L kg^{-1}) is the particulate (mg kg^{-1}) to dissolved (mg L^{-1}) concentration ratio (Equation 1). The relative contribution of the particulate concentration (X_p) of a given element X to the total (dissolved + particulate) concentration of the same element (X_T, Equation 2) is expressed as the fraction of X_p (F_p, expressed in percentage, Equation 3).

$$K_d = X_p / X_d \quad (1)$$

$$X_T = X_p \cdot SPM + X_d \quad (2)$$

$$F_p(\%) = \left(X_p \cdot SPM\right)/X_T = (K_d \cdot SPM)/(1 + K_d \cdot SPM) \quad (3)$$

where X_p is expressed in mg kg^{-1}, X_d in mg L^{-1}, X_T in mg L^{-1} and SPM in kg L^{-1}. This Kd should also match the slope of the isotherm experiments.

2.6. Adsorption isotherm models

The exchange of a substance between the dissolved and particulate phases reaches a dynamic equilibrium (i.e., equal sorption and desorption rates) after sufficient contact time (Foo and Hameed 2010). Appropriate modelling and thermodynamic considerations provide insights into the adsorption

mechanisms (i.e., physisorption vs chemisorption), surface properties and sorption strength (Foo and Hameed 2010, and references therein).

The Langmuir empirical model is the most common two-parameter isotherm employed to describe monolayer chemical saturation onto finite sites with no lateral interactions between adsorbed molecules (no "steric hindrance"; Langmuir 1918). The mathematical equation for the Langmuir isotherm (Equation 4) is complemented with the dimensionless constant (R_L) also known as the separation factor or equilibrium parameter (Equation 5) defined by Weber and Chakravorti (1974):

$$X_p = (X_{pmax} \cdot K_L \cdot X_d)/(1 + K_L \cdot X_d) \quad (4)$$

$$R_L = 1/(1 + K_L \cdot X_{d0}) \quad (5)$$

where X_p is the concentration of element X in the particulate phase at equilibrium (mg kg^{-1}), calculated from the difference in dissolved concentrations between the initial spiked (X_{d0}) and the equilibrium (X_d) concentrations (µg L^{-1}, converted to particulate concentrations with the corresponding SPM ratio), X_{pmax} is the maximum charge of X in the SPM and K_L is the constant of Langmuir (L μg^{-1}). Values of R_L indicate the adsorption nature of the isotherm as unfavourable (R_L>1; i.e., highly soluble elements), linear (R_L=1), favourable (0<R_L<1) and irreversible (R_L = 0; i.e., high affinity for the particulate phase; Weber and Chakravorti 1974).

The Freundlich empirical model was the first one to describe heterogeneous (i.e., non-uniform distribution) multilayer adsorption on a non-homogeneous surface (Freundlich 1907). The mathematical expression of the Freundlich isotherm (Equation 6) represents the adsorption intensity by the K_F constant (i.e., the higher the value the higher the affinity for the particulate phase) and the surface heterogeneity with the c value (i.e., the closer to zero the more heterogeneous; Foo and Hameed 2010). When c = 1, the relationship between X_p and X_d is linear and K_F = Kd (distribution coefficient).

$$X_p = K_F \cdot X_d^c \quad (6)$$

3. Results

3.1. Tellurium sorption kinetics and isotherms

Sorption kinetics of dissolved Te (Te_{ex}) was rapid (>40% in less than 3 min., Figure 1a) independent from salinity, but highly dependent on the solid/liquid ratios, showing ~90% sorption in 1000 mg L^{-1} SPM within 3 min. Equilibrium between the dissolved and particulate phases was achieved at ≥ 48h in 100 mg L^{-1} SPM and in <5h for 1000 mg L^{-1} SPM (Figure 1a). Experimental blanks (i.e., no SPM) showed no measurable Te_{ex} loss or adsorption onto tube walls throughout the

whole experiment duration. Estimated particulate concentrations were used to calculate partitioning coefficients for Te_{ex} at 48h of adsorption time, showing log_{10} Kd values in freshwater of 4.94 ± 0.02 L kg^{-1} for 100 mg L^{-1} and 5.31 ± 0.01 L kg^{-1} for 1000 mg L^{-1}, whereas in seawater Kd values were 4.98 ± 0.02 L kg^{-1} for 100 mg L^{-1} and 4.96 ± 0.09 L kg^{-1} for 1000 mg L^{-1}.

Sorption isotherms showed non-linear correlations at low SPM concentrations (100 mg L^{-1}, Figure 1b) following a Langmuir isotherm. Langmuir parameters were K_L = 3.91 L μg^{-1} and b = 50.7 mg kg^{-1} with a separation factor of "favourable" to "very favourable" due to R_L variations between 0.72 and 0.05. Nevertheless, higher SPM content of 1000 mg L^{-1} showed a linear behaviour representative of a Freundlich isotherm (Figure 1c) with relatively low heterogeneity (c = 1). The value of ~0.02 mg kg^{-1} at the intercept represented the inherited Te in the SPM, thus, included in the Te_p concentrations. Calculated Te_p concentrations were in accordance with directly analysed Te_p (<15% difference, within analytical error) from 1000 mg L^{-1} experimental isotherm sediments.

3.2. Selenium sorption kinetics and isotherms

Selenium sorption kinetics (Se_{ex}, Figure 2a) was less rapid than that of Te_{ex} (Figure 1a), showing <10% sorption after 3 min of exposure. There seems to be an effect of both salinity (i.e., higher sorption in seawater) and SPM concentration (i.e., higher sorption in 1000 mg L^{-1}), reaching solid/liquid equilibrium in <24h for 1000 mg L^{-1} with max. 25% sorption. Precise sorption kinetics and equilibrium time for 100 mg L^{-1} (max. 5% sorption) were uncertain, as all Se_d values were close to the experimental blank concentrations with 4% variability shown by the standard deviation. Experimental blanks showed no measurable ^{77}Se loss or adsorption onto tube walls along the experiment. Estimated log_{10} Kd values at 48h were: 2.51 ± 0.08 L kg^{-1} for 100 mg L^{-1} and 2.42 ± 0.04 L kg^{-1} for 1000 mg L^{-1} in freshwater, whereas in seawater they were 2.87 ± 0.10 L kg^{-1} for 100 mg L^{-1} and 2.57 ± 0.04 L kg^{-1} for 1000 mg L^{-1}.

Sorption isotherms for both SPM conditions (100 mg L^{-1} and 1000 mg L^{-1}) showed similar concentrations and linear correlations, representative of a Freundlich isotherm (Figure 2b). The value at the intercept of ~0.26 mg kg^{-1} represented inherited Se included in the Se_p values. Calculated Se_p concentrations tended to be ~30% higher than those directly measured for 1000 mg L^{-1} SPM isotherm samples.

3.3. Selective extractions

Selective extractions from both freshwater (S=0) and seawater (S=32) experiments of independent ^{125}Te and ^{77}Se spikes showed differences between spiked and inherited concentrations as well as

304 distinct fractionation patterns for both elements (Figure 3). Relative contributions of each extracted
305 fraction to total (inherited or spiked) Te and Se concentrations were expressed in percentages (Figure
306 3). Total concentrations used for Te calculations were 0.05 mg kg^{-1} for Te_{nat} whereas 2.68 mg kg^{-1} in
307 S=0 and 3.20 mg kg^{-1} in S=32 for respective Te_{ex} concentrations. Total Se_{nat} concentrations ranged
308 between 0.37-0.53 mg kg^{-1} and average Se_{ex} was 25.7 mg kg^{-1} in both, freshwater and seawater.

309 The acid-soluble fractions showed the highest Te_{nat} contribution (~50% in F4 and ~30% in F4N,
310 Figure 3a) for freshwater experiments and were 10-20% lower in seawater experiments. Average Te_{nat}
311 contribution was 14% in the H_2O_2 fraction (F3, associated to organic matter), <2% in both, the easily
312 exchangeable or carbonate fractions (F1) and the amorphous Mn/Fe oxide fraction (F2; Figure 3a). In
313 contrast, Te_{ex} sorbed preferentially (average ~60%) to the acid-soluble mineral phases (F4-F4N),
314 comprising amorphous and crystalline Fe and Mn oxides, carbonates, amorphous monosulphurs (e.g.,
315 acid volatile sulphides and FeS) and phyllosilicate phases. The latter also implies a ~40% retention of
316 Te_{ex} in the residual fraction. Up to 10% of Te_{ex} was sorbed in the F1-acetate (easily exchangeable or
317 carbonates fraction) and F2-ascorbate (Mn/Fe oxides) extracted fractions, obtaining a lower, <0.2%
318 extraction with the oxidisable fraction (F3-H_2O_2 organic matter and labile/amorphous sulphide
319 phases). In any case, low differences (~5%) were observed between freshwater-adsorbed and
320 seawater-adsorbed Te_{ex} except for acid-soluble fractions where this difference varied from 20 to 30%.

321 Selective extractions for Se_{nat} showed highest contributions (≥85%) in the F3-H_2O_2 fraction
322 (targeting organic matter and labile/amorphous sulphide phases) of SPM exposed to contrasting
323 salinities (Figure 3b). Acid-soluble fractions obtained from 1M HCl showed 2-fold lower Se_{nat}
324 extractions than 1M HNO_3. Ascorbate solutions extracted concentrations of Se_{nat} similar to that of
325 HCl-extracted aliquots, and the lowest Se_{nat} fractions occurred in acetate extractions (~1%, Figure 3b).
326 Spiked concentrations were also highly extracted in the F3-H_2O_2 fraction, representing 95-105% of
327 total sorbed Se_{ex}. Noteworthy, the second most important fraction was the F2-ascorbate fraction,
328 extracting ~60% of Se_{ex}, presumably from amorphous Mn/Fe oxide mineral phases. This amount of
329 Se_{ex} extracted was higher than that in the acid-soluble fractions F4 and F4N, both extracting ~20% of
330 Se_{ex}. Only 12% of Se_{ex} was leached in the easily exchangeable/carbonate fraction (F1-acetate
331 extraction). Differences between freshwater-adsorbed and seawater-adsorbed Se_{ex} were <10%.

332

333 ## 4. Discussion

334 ### 4.1. Tellurium reactivity and solid fractionation in estuarine salinity and turbidity gradients

335 Results from sorption isotherms suggest a relatively high Te affinity for the particulate phases, as
336 previously reported for Te radionuclides (Whitehead et al. 1988) and natural Te in the Changjiang
337 Estuary (Wu et al. 2014). The observed $\log_{10}$ Kd values for experimentally adsorbed Te are similar to

typical Te $\log_{10}$ Kd values in the Garonne-Gironde fluvial-estuarine system (Gil-Díaz et al. 2019a) ranging from 4.9 to 5.3 L kg^{-1}. These values are up to one order of magnitude greater than those of natural As (3.5 – 4.8 L kg^{-1}) and Sb (3.8 – 4.8 L kg^{-1}; Gil-Díaz et al. 2018) suggesting that the solubility/mobility of both natural and experimentally adsorbed Te is lower than that of natural As and Sb. Experimentally adsorbed Se showed even lower partitioning (2.4 – 2.9 L kg^{-1}, this study) with ~2 orders of magnitude lower than those of Te, suggesting that Se and Te solubility in environmental matrices may be very different.

Tellurium partitioning may also be compared to that of Cs, given (i) their potential common sources from weathering/remobilisation processes in the watershed (Gil-Díaz et al. 2019a), and (ii) their considerable radioactivity after accidental events (Steinhauser et al. 2014), making them relevant for radionuclide dispersion models. While the observed Te partitioning suggests relatively constant $\log_{10}$ Kd of ~ 4.9 L kg^{-1}, the reported Cs $\log_{10}$ Kd values range from <4.7 L kg^{-1} in river systems (Ciffroy et al. 2009) to typical values of $\log_{10}$ Kd 5.1 to 6.8 L kg^{-1} in the Garonne-Gironde fluvial system (Gil-Díaz et al. unpublished). Furthermore, Te $\log_{10}$ Kd values are similar for both freshwater and seawater matrices with a maximum decrease of only 0.3 L kg^{-1} in the seawater, similar decreases to that observed for Sb in the Gironde Estuary (i.e., 0.2 L kg^{-1}; Gil-Díaz et al. 2018). In contrast, the difference in Cs $\log_{10}$ Kd between freshwater and seawater is 1.4 L kg^{-1} under experimental conditions (Oughton et al. 1997). Therefore, one would expect only little desorption of Te along estuarine salinity gradients, compared to Cs mobilisation. This major difference in estuarine geochemical behaviour represents important information for the development of continent-ocean transition models anticipating potential Te and Cs radionuclide dispersion after accidental NPP releases. This observation also implies different biological transfers of Te and Cs, depending on the dissolved concentrations and bioaccessible fractions from the particle phase.

Assuming Te adsorption under natural conditions and at natural, low concentrations (i.e. less Te available for adsorption) one would expect the limited Te available to preferentially adsorb onto sites with high binding energy. Under experimental conditions, when relatively abundant dissolved Te exceed the number of strong binding sites, the different Te species would adsorb onto different sites, according to the respective binding strengths, starting with the high binding energy sites. However, the sorption isotherms of dissolved Te onto the particulate phase fits a Langmuir (chemisorption-driven) behaviour for both the low SPM ratio (~100 mg L^{-1}; Figure 1b) and the high SPM condition (1000 mg L^{-1}; Figure 1c), suggesting homogeneous monolayer adsorption of Te at equal bonding energy sites until saturation (Foo and Hameed 2010). This observation implies that, in the present experiment, the amount of dissolved Te available for adsorption did not exceed the number of strong bonding energy sites available, and thus may be representative of sorption processes under natural conditions. This saturation would be achieved at ~50 mg kg^{-1} for Garonne River SPM which, together with kinetic results suggest that, in the maximum turbidity zone (MTZ) of the Gironde Estuary (SPM ≥ 1000 mg L^{-}

[1]; Sottolichio and Castaing 1999), a hypothetic Te_d concentration of 50 µg L^{-1} could be retained to ~90% within <3 min. Nearly all Te_d (98%) would adsorb to the SPM in less than 2 h (Figure 1a). However, environmental concentrations of dissolved Te are found within the ultra-trace levels (e.g., Belzile and Chen 2015), and in the case of potential NPP accidents released Te masses would be expected to be orders of magnitude lower than those needed to reach saturation. In fact, a maximum of 68 000 000 Bq m^{-3} of ^{137}Cs (equivalent to ~20 ng L^{-1}) has been detected in early April in surface waters adjacent to the FDNPP, decreasing to 10 000 Bq m^{-3} (equivalent to ~3 pg L^{-1}) in early 2012 (Buesseler et al. 2017). Therefore, assuming that the amounts of Te released would be similar in magnitude (or lower) than those of ^{137}Cs, nearly all Te_d radionuclides potentially released/produced in the Gironde Estuary would be highly retained in the particulate phase, even in seawater conditions. The latter is in accordance with the scavenged behaviour of Te observed in open ocean profiles of the Pacific and Atlantic Oceans, the East China Sea and the Angola and Panama Basins (Lee and Edmond 1985; Yoon et al. 1990; Wu et al. 2014).

The F4 acid-soluble fraction (attributed to the sum of amorphous and crystalline Fe and Mn oxides, carbonates, amorphous monosulphurs and phyllosilicate phases) is commonly considered to represent the fraction potentially bioaccessible to organisms (Australian and New Zealand sediment quality guidelines; ANZECC and ARMCANZ 2000). Based on this idea, the extractions suggest that ~30% of Te_{nat} in the SPM and ~60% of the experimentally added Te_{ex} retained in the particulate phase would be potentially bioaccessible. Accordingly, these fractions could impact filter-feeding organisms such as economically relevant bivalves (i.e., oysters) with unknown implications for the food chain. Interestingly, this observation also suggests that ~40% of the experimentally adsorbed Te_{ex} could not be recovered by 1M acid extraction, i.e. would be bound to the so-called residual fraction, typically attributed to minerals that are considered as relatively insoluble under respective conditions (Gupta and Chen 1975). Adsorption of Te_{ex} to both, the bioacessible (60%) and residual (40%) fractions implies interaction with different mineral surfaces, which would not be consistent with the Te_{ex} adsorption isotherm fitting the Langmuir model, unless different fractions showed relatively similar surface properties regarding Te sorption. Differences in Te dissolution between 1M HCl (F4) and 1M HNO_3-based (F4N) extractions (~20% higher in HCl, Figure 3) observed for both naturally and experimentally-adsorbed Te, suggest that HCl may have stronger extraction efficiency than HNO_3, although previous work has reported similar stability and solubility in both HCl and HNO_3 solutions (Inorganic Ventures 2016).

Furthermore, these results appear to be in opposition with the higher Te adsorption observed in SPM in seawater conditions compared to that in freshwater (3.20 vs 2.70 mg kg^{-1}, respectively). In fact, the relatively low acid-soluble extractions obtained from SPM exposed to seawater compared to freshwater conditions suggest that Te binds somehow strongly in seawater conditions (i.e., not related to easily exchangeable binding sites). This observation is in accordance with the observed negative

410 correlation between the labile fraction of Te_p and the salinity gradient in the Changjiang Estuary (Duan
411 et al. 2014). Nevertheless, further research is required to verify these hypotheses and the specific
412 binding modes of Te to amorphous and crystalline Fe and Mn oxides, amorphous monosulphurs and
413 phyllosilicate phases.

414 Low extraction of Te_{nat} from the exchangeable/carbonate (<10% in F1), the amorphous Fe/Mn
415 oxide fraction (<10% in F2) and the organic matter fraction (~14% in F3) are consistent with Te_{nat}
416 extractions in marine SPM from the East China Sea (Duan et al. 2014). In fact, Duan et al. (2014)
417 observed 13% and 11% Te in the exchangeable and carbonates fraction (i.e., from an acetate-solution
418 extraction), 11% in the Fe–Mn oxides (i.e., from a hydroxylamine-based solution) and 15% in the
419 organic matter fraction (i.e., from H_2O_2-solution extraction), leaving ~50% in the so-called "residual"
420 fraction. Similarly, the residual fraction (accounted as the difference between total Te and that in F4)
421 of the Garonne River SPM carried ~50% in freshwater-exposed SPM and 70% in seawater-exposed
422 SPM of Te_{nat}.

423 For the experimentally adsorbed Te_{ex} simulating potential anthropogenic Te release into the natural
424 environment the results suggest that up to ~99% would be fixed onto SPM within few hours,
425 depending on SPM concentrations. After sediment deposition in the estuarine banks and bed during
426 tidal slacks, the onset of early diagenetic processes might potentially release (i) up to 10% of Te_{ex} due
427 to reductive dissolution of reactive Fe and Mn oxyhydroxides as simulated by ascorbate extractions
428 (F2), and (ii) less than 1% of Te_{ex} adsorbed to organic matter (H_2O_2 extraction, F3). The relatively low
429 F3 fraction obtained for Te_{ex} compared to that of Te_{nat} (14%) may suggest that Te physisorption or
430 chemisorption onto particulate organic matter may be smaller than Te fixation by active incorporation
431 (absorption). The observed results are applicable to Te(VI) sorption behavior, which is assumed to be
432 representative of environmental conditions as Te(VI) is generally more abundant than Te(IV) in
433 aquatic systems (Lee and Edmond 1985; Yoon et al. 1990), representing up to 5-fold the abundance of
434 Te(IV) in the Changjiang Estuary (Wu et al. 2014). The precise Te species released to the environment
435 after a NPP accident are unknown, potentially varying between events due to specific accident
436 conditions. In fact, the presence and concentration of radionuclide species in the nuclear fuel depend
437 on several factors including fuel composition and fuel burnup (Kleykamp 1985). Nevertheless, both
438 Te(IV) and Te(VI) equally adsorb to Fe(III) hydroxides and Te(IV) to illite mineral phases (Harada
439 and Takahashi 2009; Qin et al. 2017). Thus, this work may serve as a preliminary approach to
440 radionuclide Te dispersion fate scenarios in the Gironde Estuary.

441 In a scenario of Te radionuclide dispersion after hypothetical NPP accidental events the above
442 considerations suggest a dominant role of the estuarine SPM in Te retention and dispersion
443 independent from the hydrological situation. Therefore, relatively few Te radionuclides would be
444 bioavailable strongly limiting potential transfer to the atmosphere due to bio-methylation processes

(Chasteen and Bentley 2003) within the estuarine reaches. Both, relatively low (~100 mg L^{-1}) and high (>1000 mg L^{-1}) SPM concentrations would result in almost total sequestration of Te due to adsorption of Te radionuclides on suspended particles. The environmental persistence of Te radionuclides depends on both, half-lives (e.g., ranging between 3.2 days for ^{132}Te to ~3 months for ^{127m}Te for the most relevant ones) and fission yield (i.e., the probability of being produced from nuclear fission reactions). The combination of both parameters may result in estuarine Te radionuclide half-lives of several months. In any case, average particle residence times in the Gironde Estuary (1-2 years, Castaing and Jouanneau 1979), are clearly greater than the aforementioned radionuclide timescales, suggesting that the maximum decay would take place inside the estuary, except for specific hydrodynamic conditions allowing for massive particle expulsion to the coastal ocean (few days per year; Allen et al. 1980; Castaing and Allen 1981). The main decay products are radioactive or stable iodine daughter nuclides (e.g. ^{129}I with $1.57.10^7$ y half-life) which will then likely be mobilised to the water column (or pore waters) due to their relatively high solubility.

4.2. Selenium reactivity and solid fractionation in estuarine salinity and turbidity gradients

The experimentally determined sorption of Se onto SPM from the Garonne River is considerably lower than that of Te, in accordance with the mobile character of Se in aquatic systems (Fernández-Martínez and Charlet 2009). The corresponding Kd values ($\log_{10}$ Kd from 2.4 to 2.9 L kg^{-1}) are in the low Kd range of values reported for natural (stable and radioactive) Se in estuarine/coastal systems such as the San Francisco Estuary ($\log_{10}$ Kd of 2.0 – 4.5 L kg^{-1} for 100 mg L^{-1} SPM; Benoit et al. 2010) and 19 Japanese coastal regions ($\log_{10}$ Kd of 2.6 – 3.9 L kg^{-1}; Takata et al. 2016). In fact, differences between field Kd and experimental Kd for radionuclides have been also observed in environmental SPM samples (e.g., Co, Cs, Mn; Ciceri et al. 1988). These differences were explained by the contribution of the residual fraction to the calculation of field Kd (i.e., total digestions; Ciceri et al. 1988). Furthermore, Kd values are generally site-dependent as SPM mineralogy can strongly control elemental solid/liquid partitioning and Se Kd values have been observed to depend on grain size and organic matter (Takata et al. 2016). Sediments of the Gironde Estuary show characteristic particulate organic carbon (POC) contents ranging from 0.05 to 1.5% (Etcheber et al. 2007; Coynel et al. 2016) and mainly contain silts and some sands (7 - 480 µm; Coynel et al. 2016).

Marine and estuarine environments generally present higher abundances of Se(VI) over Se(IV) (Cutter 1978; Cutter and Bruland 1984; Guan and Martin 1991). The observed Se(VI) adsorption kinetics fit a pseudo-second order reaction, suggesting that the main process involving Se(VI) removal from the solution are physicochemical interactions (physisorption) with rate-limiting chemisorption surfaces (Robati 2013). This sorption pattern is in accordance with bidentate outer-sphere and monodentate inner-sphere complexes reported for selenate adsorbed on ferric-Fe(III) (hydr-)oxides

and clay minerals like kaolinite (Su and Suarez 2000; Peak and Sparks 2002; Nothstein 2016), despite the higher affinity of selenite (Se(IV)) inner-sphere complexes to these mineral phases (Hamdy and Gissel-Nielsen 1977; Hayes et al. 1987).

Such interactions are relatively weak reflecting the selective extractions results (Figure 3b), as more than half of the acid-soluble fraction (F4) is contributed by exchangeable Se forms (F1). This distribution of Se between several mineral phases is in line with Se(VI) sorption fitting Freundlich isotherms, implying heterogeneous sorption sites. In this case, stronger binding sites are occupied preferentially, decreasing the adsorption energy exponentially as they fill up (Zeldowitsch 1934). Weak interactions between dissolved Se(VI) and particle surfaces could be affected by ionic strength competition, decreasing Se(VI) sorption onto SPM (Su and Suarez 2000). However, the observed differences in Se sorption between freshwater- and seawater-exposed SPM fall within the analytical error.

Co-existing Se(IV) and Se(VI) forms may partly explain differences in parallel selective extractions of Se_{nat} and Se_{ex}. In fact, the selective extraction using oxidising reagents (i.e. the F3-H_2O_2 and the F4N-HNO_3 fractions; Figure 3c,d) generally show a high mobilisation of Se, probably due to the oxidation of Se(IV) to the more mobile Se(VI). Strong oxidants like H_2O_2, used to chemically oxidise the organic matter, as well as HNO_3 compared to HCl, can oxidise Se(IV) from carrier phases other than the target phase (Gruebel et al. 1988). Thus, although high Se content in the organic matter fraction would fit the nutrient type behaviour of Se in marine environments (e.g., Cutter and Bruland 1984, Cutter and Cutter 1995), the fact that the amount of Se extracted by H_2O_2 (F3) is close to 100% could also include Se extracted from other phases by oxidation (Figure 3), implying non-selectivity of the fractionation for Se. Sequential extractions in anoxic biofilms have also identified the non-selectivity of other oxidising reagents (NaOCl) targeting Se in the "organically-associated" fraction for several inorganic/organic Se species (Lenz et al. 2008). The non-selectivity of both, NaOCl and H_2O_2 extractions of Se was already identified for soil and sediment extractions by Gruebel et al. (1988). These observations clearly suggest that commonly applied extraction schemes (e.g., Tessier et al. 1979; Ure et al. 1993) need to be updated and/or adapted before applied to specific elements, such as Se.

It is commonly accepted that the 1M acid-soluble fraction includes mineral phases extracted in the ascorbate fraction, thus trace element concentrations in F4 should be equal to or greater than in F2 fractions (Huerta-Díaz and Morse 1990; Kostka and Luther 1994; Gasparon and Matschullat 2006). The similar Se_{nat} concentrations in both F4-HCl and F2-ascorbate fractions (Figure 3d) are in accordance with this statement, potentially suggesting that most (if not all) of the Se_{nat} in the F4-HCl fraction was extracted from the amorphous Fe/Mn oxide carrier phases (F2-ascorbate fraction). In contrast, Se_{ex} was greater in the F2-ascorbate fraction than in the acid soluble fractions (F4 and F4N,

Figure 3c). Interestingly, this effect of inversed extraction efficiency of parallel selective extractions (F2 vs F4) also occurred for both inherited and spiked Sb in the same SPM from the Garonne River (Gil-Díaz et al. 2019b). Thus, these results suggest an anomaly (compared to more commonly analysed elements such as Cd, Cu, Zn, Pb, etc.) for F2-ascorbate extractions of oxyanions like Se and Sb, but not Te. This effect could be potentially due to strong organic complexation of Se and Sb by the citrate present in the ascorbate solution, thus extracting higher Se and Sb concentrations, independently from the dissolution of the targeted mineral carrier phase (Gil-Díaz et al. 2019b). These observations suggest that reducing conditions and the presence of strong organic ligands, as occurring in sub-oxic early diagenetic conditions (Froelich et al. 1979), potentially enhance Se_{ex} solubility, compared to Se_{nat}.

Re-adsorption of Se (and As) onto non-targeted crystalline Fe hydroxides (i.e., goethite) is favoured during soil and sediment acid-based hydroxylamine extractions (reductive dissolution; Gruebel et al. 1988). Because acid 1M HCl extractions do not dissolve crystalline Fe hydroxides such as goethite and hematite (Raiswell et al. 1994), one cannot exclude Se dissolution from target minerals and re-adsorption onto non-target minerals (e.g. crystalline Fe hydroxides) in 1M HCl and 1M HNO_3 extractions. This effect implies that the estimation of the potentially bioaccessible Se fractions by acid extractions in sediments may be widely biased.

Combining the above findings, one would assume that, after a potential accidental release from NPPs in the Gironde Estuary, the majority of dissolved radioactive Se may be rapidly expulsed to the coastal ocean and <30% retention in the particulate phase of the MTZ. Given the similarities between sorption isotherms and Kd at 100 mg L^{-1} and 1000 mg L^{-1} SPM concentrations, dissolved Se probably is dominant for a wide range of SPM concentrations and dissolved radioactive Se releases. Moreover, reducing, suboxic conditions as existing in the MTZ water column (Robert et al. 2004) may further increase Se mobility due to leaching from particles subjected to early diagenetic processes.

Noteworthy, this expected dominance of dissolved Se radionuclides could enhance radioactivity transfer to the biological compartment, given the nutrient behaviour of Se (Tan et al. 2016). In fact, aquatic microorganisms naturally methylate Se as a part of their detoxifying mechanisms (Cooke and Bruland 1987). In the presence of Se radionuclides, bio-methylation processes might produce radioactive volatile Se (e.g., ^{75}Se, ^{79}Se and ^{82}Se) species which must be taken into account for accidental dispersion scenarios. Such Se methylation is a seasonal process (i.e., low in winter and quantifiable in summer) with estimated average fluxes of the order of 10^5 g y^{-1} for the Gironde Estuary (Amouroux and Donard 1997). Such methylation is species-dependent and can potentially show non-negligible atmospheric dispersion (Luxem et al. 2015).

Thus, accidental releases of dissolved Se radionuclides such as ^{75}Se (~119 d half-life), ^{79}Se (~10^5 y half-life) and ^{82}Se (~10^{19} y half-life) are expected to follow the dynamics of the estuarine water

column (e.g. estuarine water residence times of 10 to 80 days), implying (i) continuous exportation of dissolved radioactive Se to the coast during winter/high discharge conditions, (ii) bio-availability to primary producers and the related food chain, and (iii) potential seasonal production of radioactive methylated species exported to the atmosphere.

5. Conclusion

Batch experiments with bulk SPM and natural freshwater/seawater matrices simulating contrasting estuarine turbidity and salinity gradients showed different sorption kinetics, particulate affinity and solid fractionation distribution for Te and Se. Experimental results strongly suggest that the fluvial-estuarine geochemical cycles of Te and Se are not comparable in terms of reactivity, solubility and bioavailability. Further knowledge on Te speciation and sorption mechanisms is required in environmental studies.

The solid fractionation results suggest that anthropogenic releases of dissolved Te and Se to the aquatic environment do not fully mimic inherited element distribution among SPM mineral phases. The observed differences imply that (i) particulate Te_{ex} is potentially more bioaccessible than the already present particulate Te_{nat}, and that (ii) Se_{ex} may be more easily exchangeable and mobile during early diagenetic processes than Se_{nat}. Comparison of Se solid partitioning with results of selective extractions commonly applied to other trace elements point out to two anomalies: (i) enhanced dissolution of Se species in oxidising conditions probably due to oxidation of Se(IV) to the more soluble Se(VI) and subsequent mobilisation from other solid carrier phases (non-selectivity), and (ii) potential extraction by dissolved organic complexants in addition to release from reducible mineral phases. These findings clearly show that the use of commonly applied extraction schemes to other than originally tested target elements may produce artefacts that need thorough evaluation and must be taken into account for environmental interpretations.

Preliminary dispersion scenarios of hypothetical releases of Te and Se radionuclides into the Garonne-Gironde fluvial-estuarine system suggest high potential adsorption of Te radionuclides onto estuarine SPM in all hydrological conditions (flood and drought). This implies long estuarine residence times for Te radionuclides (up to several months, in accordance with the half-life and activities of the radionuclides released), and the risk of seasonal upstream movement when a hypothetic accident happens in a period when the MTZ is located downstream in the estuary. In contrast, Se radionuclides would preferentially remain in the dissolved phase continuously exported to the coastal ocean within several weeks, implying a risk of transfer to primary producers and the related food chain including seafood.

584 **Declarations of interest:** none

585

586 **Acknowledgements**

587 This study is a scientific contribution to the French National Project AMORAD (ANR-11-RSNR-
588 0002) from the National Research Agency, allocated in the framework program "Investments for the
589 Future". The authors gratefully acknowledge the financial assistance of the FEDER Aquitaine-1999-
590 Z0061, the German Academic Exchange Service DAAD and the SNF Project 200021-178784.

591

592 **References**

593 Aguerre, S., Frechou, C. (2006). Development of a radiochemical separation for selenium with the aim
594 of measuring its isotope 79 in low and intermediate nuclear wastes by ICP-MS. Talanta, 69(3),
595 565-571.

596 Allen, G. P., Salomon, J. C., Bassoullet, P., Du Penhoat, Y., De Grandpre, C. (1980). Effects of tides
597 on mixing and suspended sediment transport in macrotidal estuaries. Sedimentary Geology, 26(1-
598 3), 69-90.

599 Amouroux, D., Donard, O. F. (1997). Evasion of selenium to the atmosphere via biomethylation
600 processes in the Gironde estuary, France. Marine Chemistry, 58(1-2), 173-188.

601 ANZECC and ARMCANZ (2000). Australian and New Zealand guidelines for fresh water and marine
602 water quality. Australian and New Zealand Environment and Conservation Council/Agriculture
603 and Resource Management Council of Australia and New Zealand, Canberra

604 Audry, S., Blanc, G., Schäfer, J. (2006). Solid state partitioning of trace metals in suspended
605 particulate matter from a river system affected by smelting-waste drainage. Science of the Total
606 Environment, 363(1-3), 216-236.

607 Asai, S., Hanzawa, Y., Okumura, K., Shinohara, N., Inagawa, J., Hotoku, S., Suzuki, K., Kaneko, S.
608 (2011). Determination of 79Se and 135Cs in spent nuclear fuel for inventory estimation of high-
609 level radioactive wastes. Journal of Nuclear Science and Technology, 48(5), 851-854.

610 Baeza, A., Corbacho, J. A., Rodríguez, A., Galván, J., García-Tenorio, R., Manjón, G., Mantero, J.,
611 Vioque, I., Arnold, D., Grossi, C., Serrano, I., Vallés, I., Vargas, A. (2012). Influence of the
612 Fukushima Dai-ichi nuclear accident on Spanish environmental radioactivity levels. Journal of
613 Environmental Radioactivity, 114, 138-145.

614 Belzile, N., Chen, Y. W. (2015). Tellurium in the environment: A critical review focused on natural
615 waters, soils, sediments and airborne particles. Applied Geochemistry, 63, 83-92.

616 Benoit, M. D., Kudela, R. M., Flegal, A. R. (2010). Modeled trace element concentrations and
617 partitioning in the San Francisco estuary, based on suspended solids concentration. Environmental
618 Science and Technology, 44(15), 5956-5963.

619 Biver, M., Quentel, F., Filella, M. (2015). Direct determination of tellurium and its redox speciation at
620 the low nanogram level in natural waters by catalytic cathodic stripping voltammetry. Talanta, 144,
621 1007-1013.

Bizsel, N., Ardelan, M. V., Bizsel, K. C., Suzal, A., Demirdag, A., Sarıca, D. Y., Steinnes, E. (2017). Distribution of selenium in the plume of the Gediz River, Izmir Bay, Aegean Sea. Journal of Marine Research, 75(2), 81-98.

Bordas, F., Bourg, A. C. (1998). A critical evaluation of sample pretreatment for storage of contaminated sediments to be investigated for the potential mobility of their heavy metal load. Water, Air, and Soil Pollution, 103(1-4), 137-149.

Buesseler, K., Dai, M., Aoyama, M., Benitez-Nelson, C., Charmasson, S., Higley, K., Maderich, V., Masqué, P., Morris, P.J., Oughton, D., Smith, J. N. (2017). Fukushima Daiichi–derived radionuclides in the ocean: transport, fate, and impacts. Annual Review of Marine Science, 9, 173-203.

Castaing, P., Allen, G. P. (1981). Mechanisms controlling seaward escape of suspended sediment from the Gironde: a macrotidal estuary in France. Marine Geology, 40(1-2), 101-118.

Castaing, P., Jouanneau, J. M. (1979). Temps de résidence des eaux et des suspensions dans l'estuaire de la Gironde. Journal Recherche Océanographie IV, 41-52.

Chasteen, T. G., Bentley, R. (2003). Biomethylation of selenium and tellurium: microorganisms and plants. Chemical Reviews, 103(1), 1-26.

Ciceri, G., Traversi, A.L., Martinotti, W., Queirazza, G. (1988). Radionuclide partitioning between water and suspended matter: comparison of different methodologies. Studies in Environmental Science, 34, 353-375.

Ciffroy, P., Durrieu, G., Garnier, J. M. (2009). Probabilistic distribution coefficients (Kds) in freshwater for radioisotopes of Ag, Am, Ba, Be, Ce, Co, Cs, I, Mn, Pu, Ra, Ru, Sb, Sr and Th–implications for uncertainty analysis of models simulating the transport of radionuclides in rivers. Journal of Environmental Radioactivity, 100(9), 785-794.

Cooke, T. D., Bruland, K. W. (1987). Aquatic chemistry of selenium: evidence of biomethylation. Environmental Science and Technology, 21(12), 1214-1219.

Coynel, A., Gorse, L., Curti, C., Schafer, J., Grosbois, C., Morelli, G., Ducassou, E., Blanc, G., Maillet, G.M., Mojtahid, M. (2016). Spatial distribution of trace elements in the surface sediments of a major European estuary (Loire Estuary, France): Source identification and evaluation of anthropogenic contribution. Journal of Sea Research, 118, 77-91.

Cutter, G. A. (1978). Species determination of selenium in natural waters. Analytica Chimica Acta, 98(1), 59-66.

Cutter, G. A. (1989). The estuarine behaviour of selenium in San Francisco Bay. Estuarine, Coastal and Shelf Science, 28(1), 13-34.

Cutter, G. A., Bruland, K. W. (1984). The marine biogeochemistry of selenium: A re-evaluation. Limnology and Oceanography, 29(6), 1179-1192.

Cutter, G. A., Cutter, L. S. (1995). Behavior of dissolved antimony, arsenic, and selenium in the Atlantic Ocean. Marine Chemistry, 49(4), 295-306.

Duan, L. Q., Song, J. M., Yuan, H. M., Li, X. G., Li, N., Ma, J. K. (2014). Distribution, chemical speciation and source of trace elements in surface sediments of the Changjiang Estuary. Environmental Earth Sciences, 72(8), 3193-3204.

662 Edwards, J.O., Abbott, J.R., Ellison, H.R. and Nyberg, J. (1959). Coördination Number Changes
663 during Oxidation-Reduction Reactions of Oxyanions. The Kinetics of the Aniline Nitrosation and
664 of the Glycol–Tellurate Reaction. The Journal of Physical Chemistry, 63(3), 359-365.

665 Element Collection Inc.: Gray, T., Mann, N., Whitby, M. (2007). Periodic Table of Isotopes.
666 http://periodictable.com/Isotopes/051.123/index.p.full.html (accessed on the 10 March 2015)

667 Etcheber, H., Taillez, A., Abril, G., Garnier, J., Servais, P., Moatar, F., Commarieu, M. V. (2007).
668 Particulate organic carbon in the estuarine turbidity maxima of the Gironde, Loire and Seine
669 estuaries: origin and lability. Hydrobiologia, 588(1), 245-259.

670 Fernández-Martínez, A., Charlet, L. (2009). Selenium environmental cycling and bioavailability: a
671 structural chemist point of view. Reviews in Environmental Science and Bio/Technology, 8(1), 81-
672 110.

673 Filella, M. (2013). Food for thought: a critical overview of current practical and conceptual challenges
674 in trace element analysis in natural waters. Water, 5(3), 1152-1171.

675 Filella, M., Rodushkin, I. (2018). A concise guide for the determination of less-studied technology-
676 critical elements (Nb, Ta, Ga, In, Ge, Te) by inductively coupled plasma mass spectrometry in
677 environmental samples. Spectrochimica Acta Part B: Atomic Spectroscopy, 141, 80-84.

678 Foo, K. Y., Hameed, B. H. (2010). Insights into the modeling of adsorption isotherm systems.
679 Chemical Engineering Journal, 156(1), 2-10.

680 Freundlich, H. (1907). Über die adsorption in lösungen. Zeitschrift für physikalische Chemie, 57(1),
681 385-470. [Over the adsorption in solution, Journal of Physical Chemistry, 57, 385–471.]

682 Froelich, P., Klinkhammer, G. P., Bender, M. L., Luedtke, N. A., Heath, G. R., Cullen, D., Dauphin,
683 P., Hammond, D., Hartman, B., Maynard, V. (1979). Early oxidation of organic matter in pelagic
684 sediments of the eastern equatorial Atlantic: suboxic diagenesis. Geochimica et Cosmochimica
685 Acta, 43(7), 1075-1090.

686 Gasparon, M., Matschullat, J. (2006). Trace metals in Antarctic ecosystems: results from the
687 Larsemann Hills, East Antarctica. Applied Geochemistry, 21(9), 1593-1612.

688 Gil-Díaz, T., Schäfer, J., Coynel, A., Bossy, C., Dutruch, L., Blanc, G. (2018). Antimony in the Lot–
689 Garonne river system: a 14-year record of solid–liquid partitioning and fluxes. Environmental
690 Chemistry. DOI: 10.1071/EN17188

691 Gil-Díaz, T., Schäfer, J., Dutruch, L., Bossy, C., Pougnet, F., Abdou, M., Lerat-Hardy, A., Pereto, C.,
692 Derriennic, H., Briant, N., Sireau, T., Knoery, J., Blanc, G. (2019a). Tellurium behaviour in a
693 major European fluvial-estuarine system (Gironde, France): fluxes, solid/liquid partitioning, and
694 bioaccumulation in wild oysters. Environmental Chemistry. DOI: 10.1071/EN18226

695 Gil-Díaz, T., Schäfer, J., Filella, M., Dutruch, L., Bossy, C. (2019b). Fractionation of inherited and
696 spiked antimony (Sb) in fluvial/estuarine bulk sediments: Unexpected anomalies in parallel
697 selective extraction protocols. Applied Geochemistry, 108, 104386 (DOI:
698 10.1016/j.apgeochem.2019.104386)

699 Gruebel, K. A., Leckie, J. O., Davis, J. A. (1988). The feasibility of using sequential extraction
700 techniques for arsenic and selenium in soils and sediments. Soil Science Society of America
701 Journal, 52(2), 390-397.

702 Guan, D. M., Martin, J. M. (1991). Selenium distribution in the Rhone delta and the Gulf of Lions.
703 Marine Chemistry, 36(1-4), 303-316

Gupta, S. K., Chen, K. Y. (1975). Partitioning of trace metals in selective chemical fractions of nearshore sediments. Environmental Letters, 10(2), 129-158.

Hamed, M. M., Holiel, M., El-Aryan, Y. F. (2017). Removal of selenium and iodine radionuclides from waste solutions using synthetic inorganic ion exchanger. Journal of Molecular Liquids, 242, 722-731.

Hamdy, A. A., Gissel-Nielsen, G. (1977). Fixation of selenium by clay minerals and iron oxides. Zeitschrift für Pflanzenernährung und Bodenkunde, 140(1), 63-70.

Harada, T., Takahashi, Y. (2009). Origin of the difference in the distribution behavior of tellurium and selenium in a soil–water system. Geochimica et Cosmochimica Acta, 72(5), 1281-1294.

Hayes, K. F., Roe, A. L., Brown, G. E., Hodgson, K. O., Leckie, J. O., Parks, G. A. (1987). In situ X-ray absorption study of surface complexes: Selenium oxyanions on α-FeOOH. Science, 238(4828), 783-786.

Horner, H. J., Leonard Jr, G. W. (1952). Preparation of Telluric Acid. Journal of the American Chemical Society, 74(14), 3694-3694.

Huerta-Díaz, M. A., Morse, J. W. (1990). A quantitative method for determination of trace metal concentrations in sedimentary pyrite. Marine Chemistry, 29, 119-144.

Inorganic Ventures (2016). https://www.inorganicventures.com (accessed on the 28 July 2018). Ishikawa, T. (2014). A brief review of dose estimation studies conducted after the Fukushima Daiichi Nuclear Power Plant accident. Radiation Emergency Medicine, 3, 21-27.

Izrael, Y.A. (2002). Radioactive fallout after nuclear explosions and accidents. Elsevier, Saint Louis.Kersten, M., Förstner, U. (1987). Cadmium associations in freshwater and marine sediment, in: Nriagu, J.O., Sprague, J.B. (Eds.), Cadmium in the Aquatic Environment, John Wiley & Sons, Inc., pp. 51-88.

Kleykamp, H. (1985). The chemical state of the fission products in oxide fuels. Journal of Nuclear Materials, 131(2-3), 221-246.

Kostka, J. E., Luther III, G. W. (1994). Partitioning and speciation of solid phase iron in saltmarsh sediments. Geochimica et Cosmochimica Acta, 58(7), 1701-1710.

Langmuir, I. (1918). The adsorption of gases on plane surfaces of glass, mica and platinum. Journal of the American Chemical Society, 40(9), 1361-1403.

Lenz, M., Hullebusch, E. D. V., Farges, F., Nikitenko, S., Borca, C. N., Grolimund, D., Lens, P. N. (2008). Selenium speciation assessed by X-ray absorption spectroscopy of sequentially extracted anaerobic biofilms. Environmental Science and Technology, 42(20), 7587-7593.

Leppänen, A. P., Mattila, A., Kettunen, M., Kontro, R. (2013). Artificial radionuclides in surface air in Finland following the Fukushima Dai-ichi nuclear power plant accident. Journal of Environmental Radioactivity, 126, 273-283.

Lee, D. S., Edmond, J. M. (1985). Tellurium species in seawater. Nature, 313(6005), 782.

Luxem, K. E., Vriens, B., Wagner, B., Behra, R., Winkel, L. H. (2015, April). Selenium uptake and volatilization by marine algae. In EGU General Assembly Conference Abstracts (Vol. 17).

Ma, Y., Uren, N.C., (1995). Application of a new fractionation scheme for heavy metals in soils. Communications in Soil Science and Plant Analysis, 26, 3291-3303.

744 Measures, C. I., Burton, J. D. (1978). Behaviour and speciation of dissolved selenium in estuarine
745 waters. Nature, 273(5660), 293.

746 Morewitz, H. A. (1981). Fission product and aerosol behavior following degraded core accidents.
747 Nuclear Technology, 53(2), 120-134.

748 Nothstein, A. K. (2016). Selenium Transfer between Kaolinite or Goethite Surfaces, Nutrient Solution
749 and Oryza Sativa (Vol. 41). KIT Scientific Publishing.

750 Oughton, D. H., Børretzen, P., Salbu, B., Tronstad, E. (1997). Mobilisation of 137Cs and 90Sr from
751 sediments: potential sources to arctic waters. Science of the Total Environment, 202(1-3), 155-165.

752 Peak, D., Sparks, D. L. (2002). Mechanisms of selenate adsorption on iron oxides and hydroxides.
753 Environmental Science and Technology, 36(7), 1460-1466.

754 Qin, H.-B, Takeichi, Y., Nitani, H., Terada, Y., Takahashi, Y. (2017). Tellurium distribution and
755 speciation in contaminated soils from abandoned mine tailings: comparison with selenium.
756 Environmental Science and Technology, 51(11), 6027-6035.

757 Raiswell, R., Canfield, D.E., Berner, R.A., (1994). A comparison of iron extraction methods for the
758 determination of degree of pyritization and the recognition of iron-limited pyrite formation.
759 Chemical Geology, 111, 101-110.

760 Robati, D. (2013). Pseudo-second-order kinetic equations for modeling adsorption systems for
761 removal of lead ions using multi-walled carbon nanotube. Journal of Nanostructure in Chemistry,
762 3(1), 55.

763 Robert, S., Blanc, G., Schäfer, J., Lavaux, G., Abril, G. (2004). Metal mobilization in the Gironde
764 Estuary (France): the role of the soft mud layer in the maximum turbidity zone. Marine Chemistry,
765 87(1-2), 1-13.

766 Saegusa, J., Kikuta, Y., Akino, H. (2013). Observation of gamma-rays from fallout collected at
767 Ibaraki, Japan, during the Fukushima nuclear accident. Applied Radiation and Isotopes, 77, 56-60.

768 Schäfer, J., Blanc, G., Lapaquellerie, Y., Maillet, N., Maneux, E., Etcheber, H. (2002). Ten-year
769 observation of the Gironde tributary fluvial system: fluxes of suspended matter, particulate organic
770 carbon and cadmium. Marine Chemistry, 79, 229-242.

771 Sonzogni, A.A. (2013). Chart of Nuclides NuDat 2.6 - National Nuclear Data Center. Brookhaven
772 National Laboratory. http://www.nndc.bnl.gov/nudat2/reCenter.jsp?z=51&n=68 (accessed on the
773 10 March 2015).

774 Sottolichio, A., Castaing, P. (1999). A synthesis on seasonal dynamics of highly-concentrated
775 structures in the Gironde estuary. Comptes Rendus de l'Académie des Sciences-Series IIA-Earth
776 and Planetary Science, 329(11), 795-800.

777 Steinhauser, G., Brandl, A., Johnson, T.E. (2014). Comparison of the Chernobyl and Fukushima
778 nuclear accidents: A review of the environmental impacts. Science of the Total Environment, 470-
779 471, 800-817.

780 Su, C., Suarez, D. L. (2000). Selenate and selenite sorption on iron oxides an infrared and
781 electrophoretic study. Soil Science Society of America Journal, 64(1), 101-111.

782 Sung, W. (1995). Some observations on surface partitioning of Cd, Cu and Zn in estuaries.
783 Environmental Science and Technology, 29, 1303.

784 Tan, L. C., Nancharaiah, Y. V., van Hullebusch, E. D., Lens, P. N. (2016). Selenium: environmental
785 significance, pollution, and biological treatment technologies. Biotechnology Advances, 34(5),
786 886-907.

787 Takata, H., Aono, T., Tagami, K., Uchida, S. (2016). A new approach to evaluate factors controlling
788 elemental sediment–seawater distribution coefficients (Kd) in coastal regions, Japan. Science of the
789 Total Environment, 543, 315-325.

790 Tessier, A., Campbell, P. G., Bisson, M. (1979). Sequential extraction procedure for the speciation of
791 particulate trace metals. Analytical Chemistry, 51(7), 844-851.

792 Ure, A. M., Quevauviller, P., Muntau, H., Griepink, B. (1993). Speciation of heavy metals in soils and
793 sediments. An account of the improvement and harmonization of extraction techniques undertaken
794 under the auspices of the BCR of the Commission of the European Communities. International
795 Journal of Environmental Analytical Chemistry, 51(1-4), 135-151.

796 Van Dael, P., Lewis, J. and Barclay, D. (2004). Stable isotope-enriched selenite and selenate tracers
797 for human metabolic studies: a fast and accurate method for their preparation from elemental
798 selenium and their identification and quantification using hydride generation atomic absorption
799 spectrometry. Journal of Trace Elements in Medicine and Biology, 18(1), 75-80.

800 Weber, T. W., Chakravorti, R. K. (1974). Pore and solid diffusion models for fixed-bed adsorbers.
801 American Institute of Chemical Engineers Journal, 20(2), 228-238.

802 Whitehead, N. E., Ballestra, S., Holm, E., Huynh-Ngoc, L. (1988). Chernobyl radionuclides in
803 shellfish. Journal of Environmental Radioactivity, 7(2), 107-121.

804 Winkel, L. H. (2016). The global biogeochemical cycle of selenium: Sources, fluxes and the influence
805 of climate. In Global Advances in Selenium Research from Theory to Application: Proceedings of
806 the 4th International Conference on Selenium in the Environment and Human Health (pp. 3-4).
807 CRC Press/Balkema.

808 Wu, X., Song, J., Li, X. (2014). Occurrence and distribution of dissolved tellurium in Changjiang
809 River estuary. Chinese Journal of Oceanology and Limnology, 32(2), 444-454.

810 Yoon, B. M., Shim, S. C., Pyun, H. C., Lee, D. S. (1990). Hydride generation atomic absorption
811 determination of tellurium species in environmental samples with in situ concentration in a graphite
812 furnace. Analytical Sciences, 6(4), 561-566.

813 Zeldowitsch, J. (1934). Adsorption site energy distribution. Acta Physicochimica URSS, 1, 961-973.

814

Figure captions:

Figure 1. Sorption of tellurium in natural SPM. (a) Te sorption kinetics (N=3) in freshwater (empty symbols) and seawater (filled symbols) matrices for 100 mg L^{-1} (triangles) and 1000 mg L^{-1} (circles) SPM content. Adsorption percentages are calculated as the difference between initial spiking concentration and Te_d at each sampling time. Tellurium isotherms (N=2, after 48h equilibration) for (b) freshwater sorption in 100 mg L^{-1} and (c) 1000 mg L^{-1} SPM content, are also shown. Curves and equations correspond to respective fitting regressions. Error bars correspond to standard deviations (SD).

Figure 2. Sorption of selenium in natural SPM. (a) Se sorption kinetics (N=3) in freshwater (empty symbols) and seawater (filled symbols) matrices for 100 mg L^{-1} and 1000 mg L^{-1} SPM content as well as (b) selenium freshwater sorption isotherms (N=2, after 48h equilibration) in 100 mg L^{-1} (triangles) and 1000 mg L^{-1} (circles) SPM content. Adsorption percentages are calculated as the difference between initial spiking concentration and Se_d at each sampling time. Curves and equations correspond to respective fitting regressions. Error bars correspond to standard deviations (SD).

Figure 3. Parallel selective extractions of Te and Se. (a) Distribution of natural Te (Te_{nat}, N=3), (b) spiked Te (Te_{ex}, N=3), (c) natural Se (Se_{nat}, N=3) and (d) spiked Se (Te_{ex}, N=1) in selective extractions after sorption in freshwater (S=0) and seawater (S=32) conditions. Targeted parallel operationally-defined solid-phase fractions were: F1 – easily exchangeable and/or carbonate fraction (acetate extraction), F2 – reducible Fe/Mn oxides (ascorbate extraction), F3 – oxidisable fraction (H_2O_2 extraction) and F4 – reactive and potentially bioaccessible fraction (HCl 1 M extraction as F4 and HNO_3 1M extraction as F4N). Percentages represent the extracted concentration in each fraction compared to total particulate concentration. Error bars correspond to standard deviations (SD).

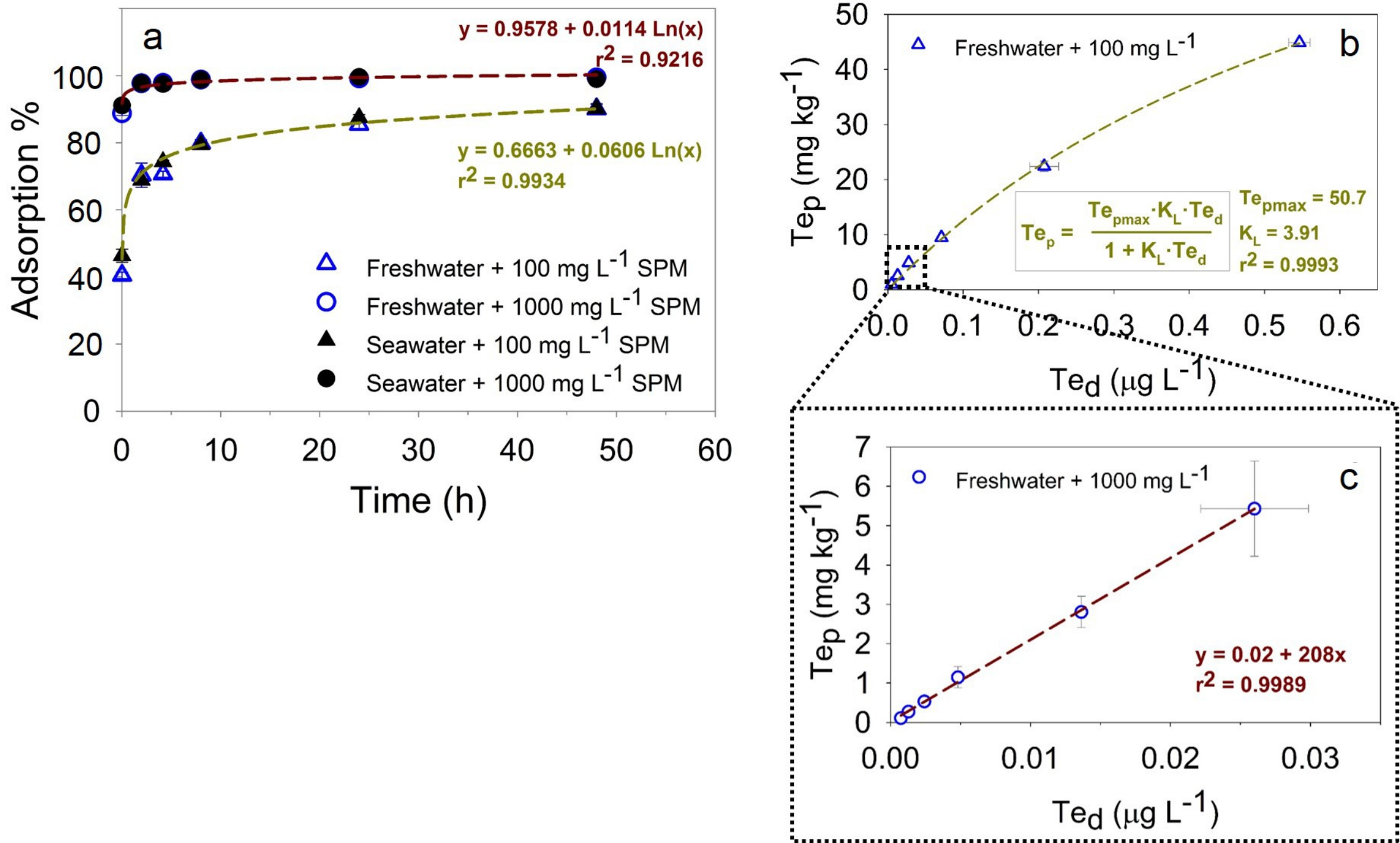
a
y = 0.9578 + 0.0114 Ln(x)
r2 = 0.9216
y = 0.6663 + 0.0606 Ln(x)
r2 = 0.9934
Freshwater + 100 mg L-1 SPM
Freshwater + 1000 mg L-1 SPM
Seawater + 100 mg L-1 SPM
Seawater + 1000 mg L-1 SPM
Adsorption %
Time (h)
b
Freshwater + 100 mg L-1
Tep (mg kg-1)
Ted (µg L-1)
Tep = Tepmax·KL·Ted / 1 + KL·Ted
Tepmax = 50.7
KL = 3.91
r2 = 0.9993
c
Freshwater + 1000 mg L-1
y = 0.02 + 208x
r2 = 0.9989

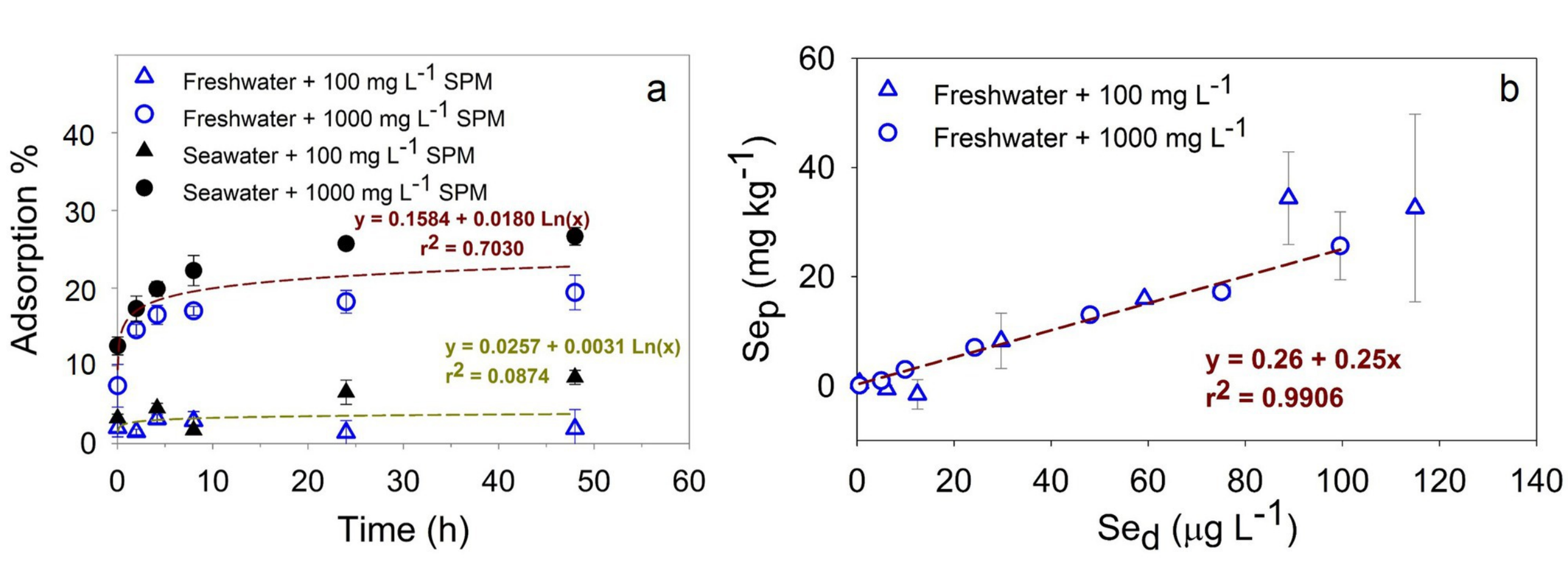
a
Freshwater + 100 mg L-1 SPM
Freshwater + 1000 mg L-1 SPM
Seawater + 100 mg L-1 SPM
Seawater + 1000 mg L-1 SPM
y = 0.1584 + 0.0180 Ln(x)
r2 = 0.7030
y = 0.0257 + 0.0031 Ln(x)
r2 = 0.0874
Adsorption %
Time (h)
0
10
20
30
40
50
60
b
Freshwater + 100 mg L-1
Freshwater + 1000 mg L-1
y = 0.26 + 0.25x
r2 = 0.9906
Sep (mg kg-1)
Sed (µg L-1)
0
20
40
60
80
100
120
140

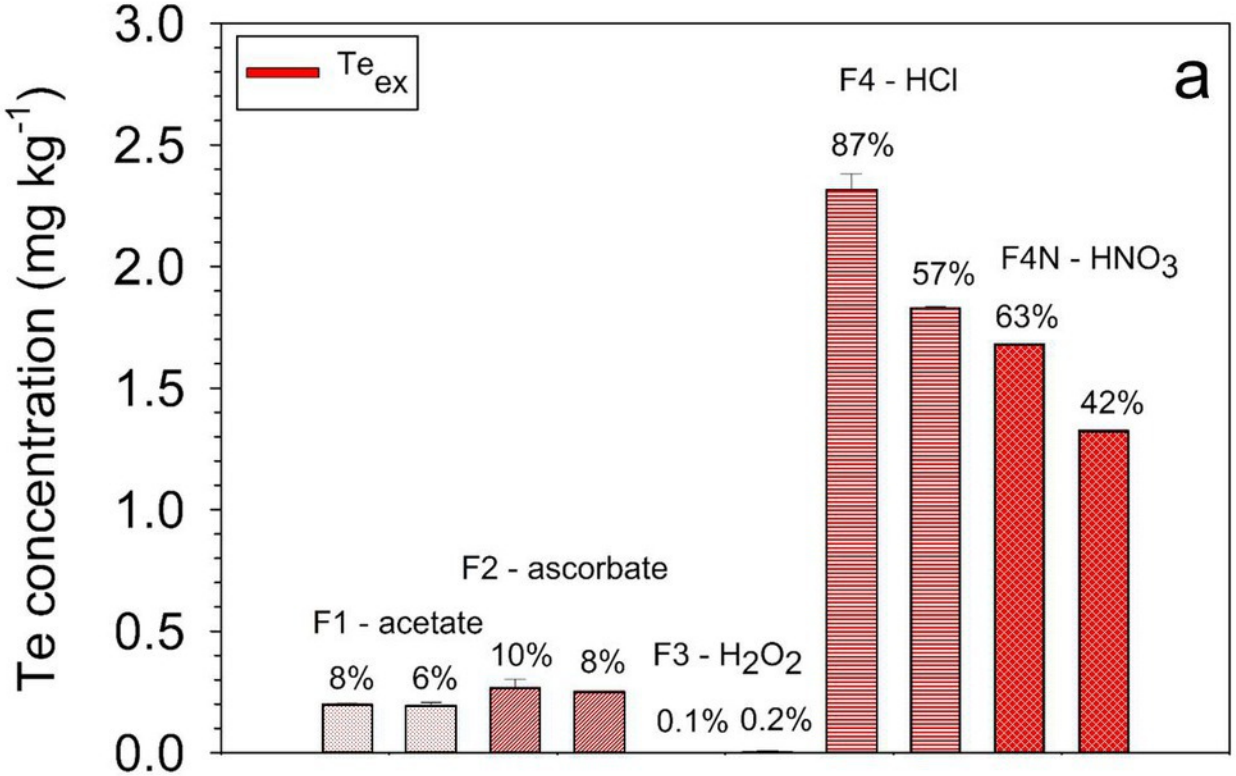
a
Te$_{ex}$
Te concentration (mg kg^{-1})
3.0
2.5
2.0
1.5
1.0
0.5
0.0
F1 - acetate
F2 - ascorbate
F3 - H$_2$O$_2$
F4 - HCl
F4N - HNO$_3$
8%
6%
10%
8%
0.1%
0.2%
87%
57%
63%
42%

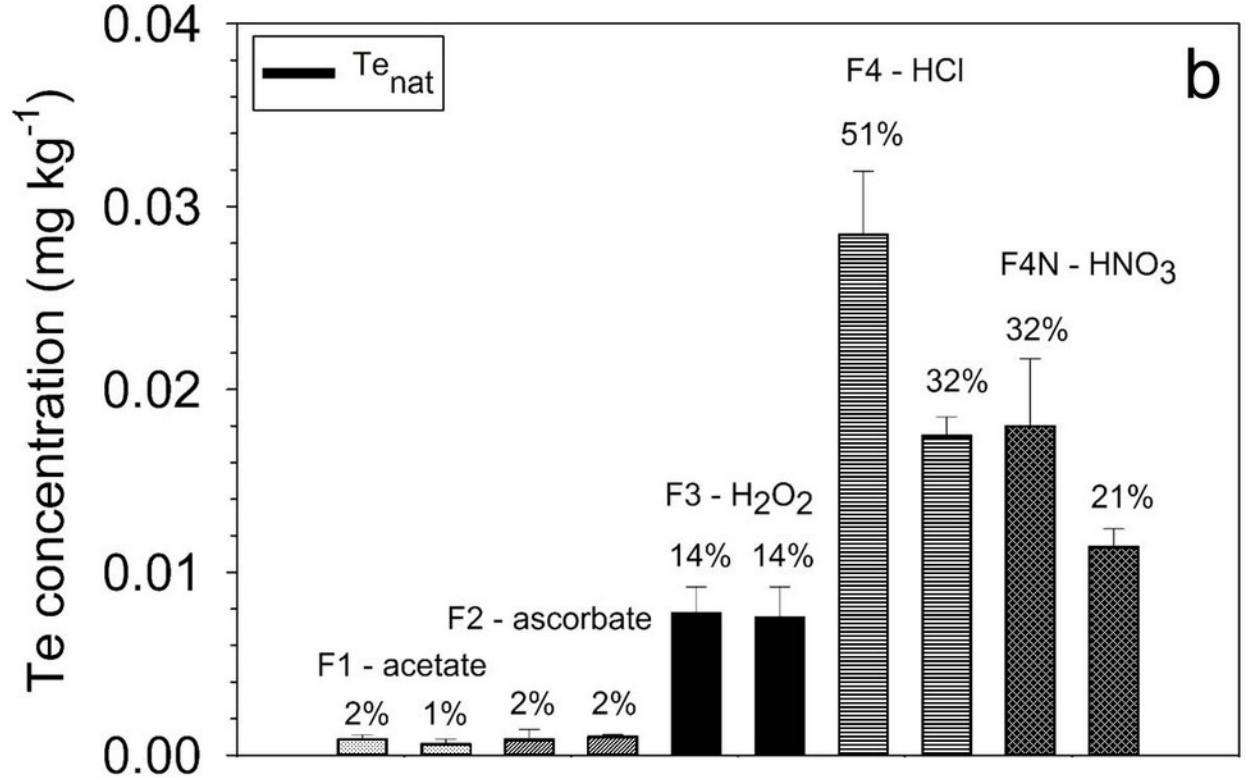
b
Te$_{nat}$
Te concentration (mg kg^{-1})
0.04
0.03
0.02
0.01
0.00
F1 - acetate
F2 - ascorbate
F3 - H$_2$O$_2$
F4 - HCl
F4N - HNO$_3$
2%
1%
2%
2%
14%
14%
51%
32%
32%
21%

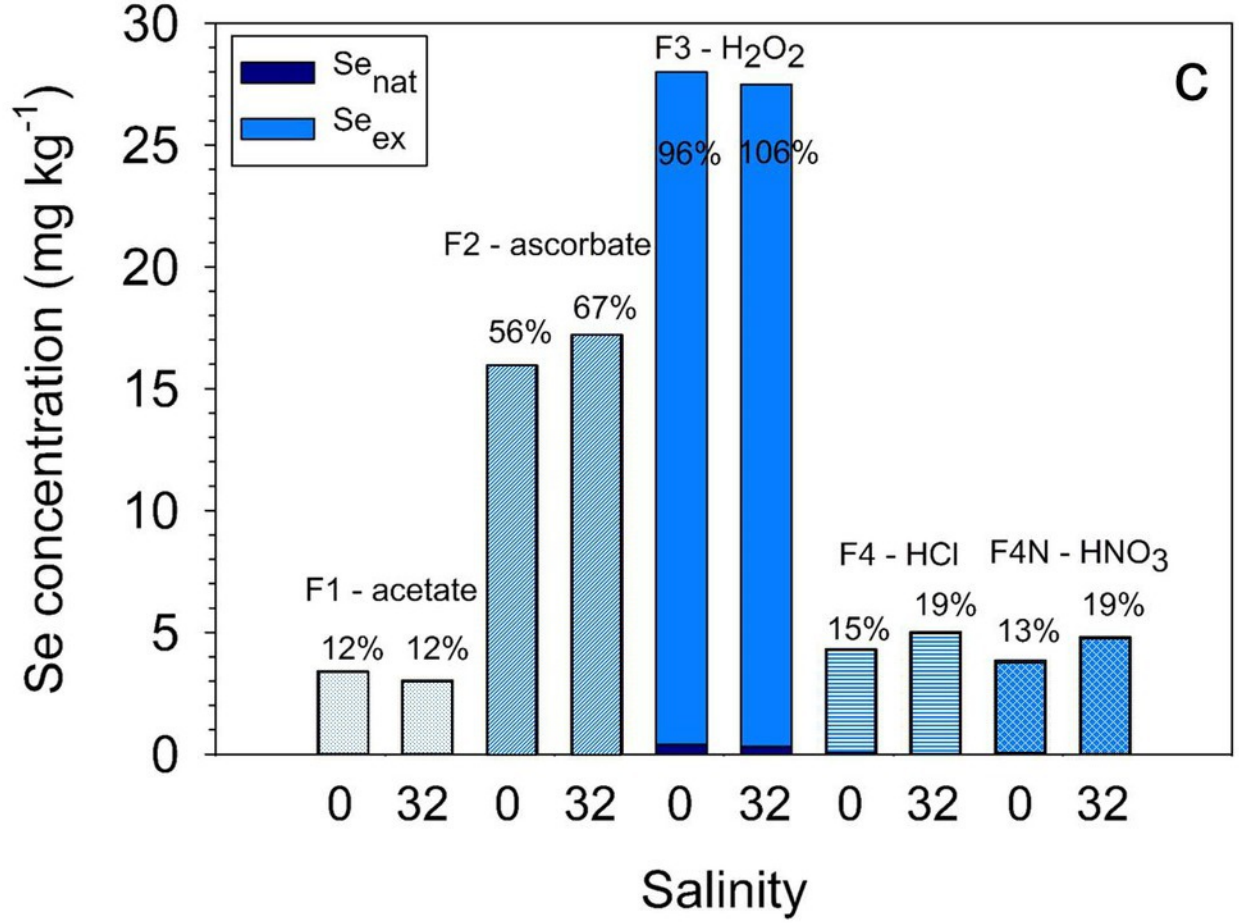
c
Se$_{nat}$
Se$_{ex}$
Se concentration (mg kg^{-1})
30
25
20
15
10
5
0
F1 - acetate
F2 - ascorbate
F3 - H$_2$O$_2$
F4 - HCl
F4N - HNO$_3$
12%
12%
56%
67%
96%
106%
15%
19%
13%
19%
0
32
Salinity

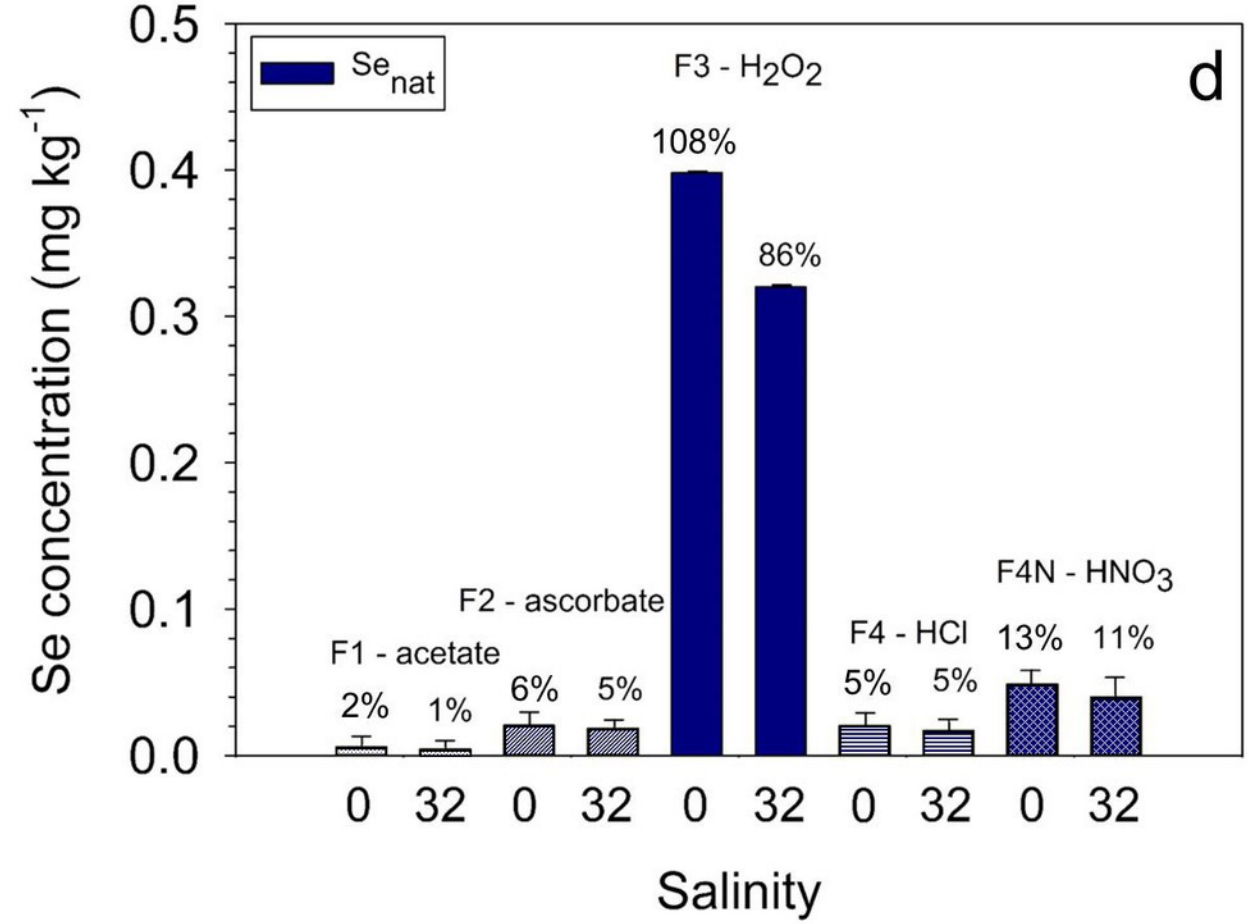
d
Se$_{nat}$
Se concentration (mg kg^{-1})
0.5
0.4
0.3
0.2
0.1
0.0
F1 - acetate
F2 - ascorbate
F3 - H$_2$O$_2$
F4 - HCl
F4N - HNO$_3$
2%
1%
6%
5%
108%
86%
5%
5%
13%
11%
0
32
Salinity

Table 1: Parallel selective extractions as described in Audry et al. (2006).

Sediment fraction	Sample weight (mg)	Reagents	Procedure
F1 – Acetate extraction (easily exchangeable and/or carbonate fraction = carbonates + Mn oxyhydroxydes + sulphates + organic matter)	500	10 ml of sodium acetate (NaOAc, 1 M) + pH adjustment with acetic acid (HOAc, 5 M) during extraction	6 h shaking at 25ºC
F2 – Ascorbate extraction (reducible Fe/Mn oxides = Mn oxides and amorphous Fe oxides)	200	12.5 ml ascorbate solution (pH = 8)	24 h shaking at 25ºC
F3 – H_2O_2 extraction (oxidisable fraction = organic matter and labile/amorphous sulphides)	500	2.5 ml H_2O_2 30% (at pH 5 with NaOH) + 1.5 ml H_2O_2 30% + 2.5 ml ammonium acetate (1M)	2 h + 3 h at 85ºC + 30 min shaking at 25ºC
F4 – acid soluble HCl extraction *(and complementary F4N – HNO_3 extraction)* (reactive and potentially bioaccessible = amorphous and crystalline Fe/Mn oxides + carbonate fractions + amorphous monosulphurs + phyllosilicates)	200	12.5 ml HCl or HNO_3 (Suprapur®, 1 M)	24 h shaking at 25ºC